03,05

Mössbauer studies of hexagonal isotropic polycrystalline ferrites $SrFe_{12}O_{19}$, received by methods of radiation-thermal sintering

© V.G. Kostishin[1], A.V. Trukhanov[1], A.A. Alekseev[2], S.V. Shcherbakov[2], I.M. Isaev[1], A.Yu. Mironovich[1], M.A. Mikhailenko[3], M.A. Sysoev[1], G.A. Skorlupin[1], G.M. Tokin[1,2]

[1] Federal State Autonomous Educational Institution of Higher Education „National Research Technology University „MISIS“, Moscow, Russia
[2] Joint Stock Company „Scientific and Production Enterprise „Istok“ named after A.I. Shokin“, Fryazino, Russia
[3] Institute of Solid State Chemistry and Mechanochemistry, Siberian Branch, Russian Academy of Sciences, Krasnoyarsk, Russia

E-mail: drvgkostishyn@mail.ru

Received November 30, 2024
Revised December 3, 2024
Accepted December 5, 2024

Hexagonal strontium ferrite ($SrFe_{12}O_{19}$) is widely used as permanent magnets and in microwave electronics. Its functional characteristics depend on the manufacturing technology. This paper for the first time uses the method of radiation-thermal sintering (RTS) in a beam of fast neutrons on ILU-6 accelerator to produce specimens $SrFe_{12}O_{19}$. The process temperature varied from 1200 to 1400°C, and sintering time — from 10 to 90 min. The phase composition and parameters of the crystalline lattice of the specimens were researched using methods of Mössbauer spectroscopy and X-ray diffraction. Mössbauer spectra were recorded on MC1104E spectrometer, and X-ray ones — on DRON-8 diffractometer. The density of the specimens is determined by Archimedes on electronic scale UW620H. The results demonstrated that all specimens are single-phase and have space group P63/mmc (№ 194), which corresponds to the structure of the hexagonal ferrite. Optimal parameters for synthesis of isotropic hexaferrites make 1250−1300°C and sintering time 30−60 min. Therefore, RTS may serve as an alternative technology to produce polycrystalline isotropic hexagonal ferrite $SrFe_{12}O_{19}$, demonstrating high energy efficiency and cost-effectiveness compared to the conventional methods

Keywords: radiation-thermal sintering, isotropic polycrystalline hexagonal ferrites $SrFe_{12}O_{19}$, crystalline structure, Mössbauer spectroscopy, elemental cell, ceramic technology, fast neutrons, electron accelerator.

DOI: 10.61011/PSS.2024.12.60210.333

1. Introduction

Hexagonal strontium ferrite of M-type $SrFe_{12}O_{19}$ (SrM) has crystalline structure, isomorphic to magnetoplumbit $PbFe_{12}O_{19}$ [1]. As a result of the difference in the values of ion radii of barium and strontium, replacement of the first ion to the second one in the crystalline lattice of hexagonal ferrite causes increase in the constant of magnetic crystallographic anisotropy K_1 by 10% [2]. Besides, SrM hexaferrites have better manufacturability compared to BaM hexaferrites [2].

Thanks to the complex of its magnetic properties and operating parameters, SrM ferrite found wide application as permanent magnets [1,2], active media of microwave electronics instruments of the mm-range of wavelengths [3] and in terahertz photonics [4]. The scientific and engineering circles are still interested in the development of microwave electronics devices based on thick films of hexagonal ferrites [5,6].

Currently the industrial method to produce the specified materials is the ceramic technology [1,2,5]. The specific process chart for production of isotropic hexagonal SrM ferrites using the ceramic technology is presented in Figure 1. Apart from some generally recognized advantages, the ceramic technology has certain disadvantages. One of the main disadvantages is — high energy capacity of this technology.

The alternative technology to produce SrM hexaferrites may be the technology of radiation-thermal sintering (RTS), which has been tested well on a few types of ferrites [7–9], including barium hexaferrite BaM [7]. The difference of the RTS technology from the traditional ceramic technology (Figure 1) consists in the fact that the operation of the thermal sintering of raw blanks is replaced with the sintering operation in a beam of fast electrons in an electron accelerator [7–9].

The objective of this paper was to study the possibility to produce quality isotropic hexaferrites $SrFe_{12}O_{19}$ using RTS technology, and to study the crystalline and magnetic

structure of the produced specimens using the X-ray diffractometry and Mössbauer spectroscopy methods.

2. Objects and methods of research

The initial specimens were prepared from oxide Fe_2O_3 of grade MM-2 (TU6-09-4816-80; impurity content SiO_2, Al_2O_3, Cr_2O_3 and Na_2O was 0.01 wt.% for each compound). Raw stock containing strontium was strontium carbonate of crystalline grade „P“ (99.0% purity) by Ispharinsky Chemical Factory. Raw blanks were prepared according to the diagram in Figure 1.

All operations, except for thermal sintering operation, were used. The operation of thermal sintering in a furnace (annealing) was replaced with RTS. The replacement of the ordinary thermal sintering for RTS in a beam of fast electrons is due to substantially lower energy capacity of the latter and higher sintering quality [7–9].

RTS of specimens was carried out using fast electrons on linear accelerator ILU-6 for radiation technology for energy 2.5 MeV G.I. Budker Institute of Nuclear Physics, Siberian Branch of the Russian Academy of Sciences [10]. The schematic diagram of this accelerator is shown in Figure 2.

Find below the main characteristics of ILU-6 accelerator:

- maximum electron energy — 2.5 MeV;
- resonant cavity operating frequency — 117 MHz;
- pulse power of HF generator — up to 2.5 MW;
- maximum pulse current of beam — 450 mA;
- maximum average current of beam — 8 mA;
- duration of beam current pulse — 0.5 ms;
- pulse repetition rate — up to 50 Hz;
- height of vacuum tank of ILU-accelerator together with HF generator — more than 2 m;
- output window length — 980 mm;
- irradiation area width — 90 cm;
- electron beam capacity released to atmosphere — up to 16 kW.

To sinter hexagonal ferrites in a beam of fast neutrons, the paper used a cell for RTS of ferrite ceramics and ferrite products designed at the department of Electronics Materials Technology, MISIS University [11].

Mössbauer spectra of study objects were registered using spectrometer MC-1104E with permanent acceleration at room temperature, the source of γ-radiation was Co^{57} in the chromium matrix. The isomer (chemical) shift was calculated relative to α-Fe. Powder samples from ground isotropic strontium hexaferrites were used for measurement. Mathematical processing of spectra was carried out using software „Univem Ms“.

X-ray phase and X-ray diffraction analysis of the study objects was carried out on DRON-8 X-ray diffractometer (made by: Russia, JSC NPP „Burevestnik“, St. Petersburg). CoK_{α_1}-radiation was used for X-ray phase analysis. Wavelength $\lambda = 0.178897$ nm. Focusing was performed using Bragg–Brentano method with two Soller slits. Measurements were done at room temperature.

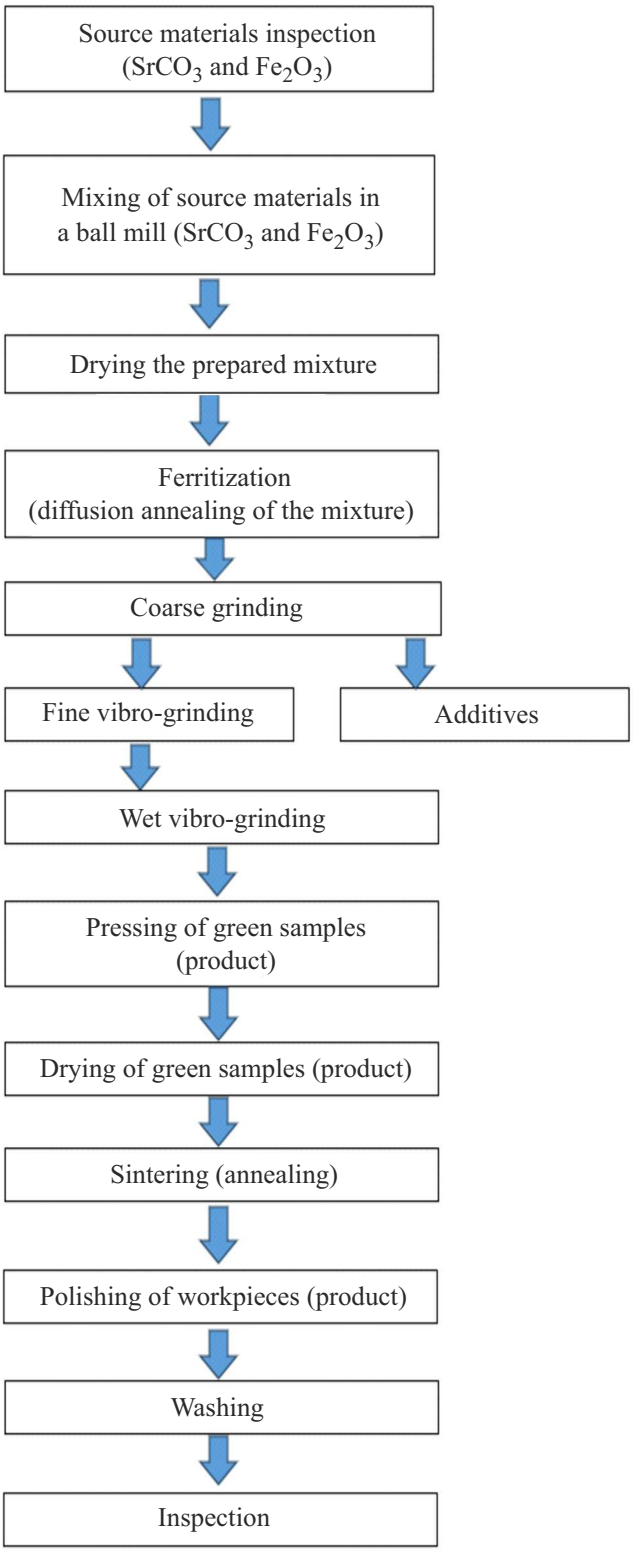

Figure 1. The specific process chart for production of isotropic hexagonal ferrites $SrFe_{12}O_{19}$ using the ceramic technology.

Estimation of the average size (L_C) of coherent scattering regions for the identified phases of all specimens studied in the paper was carried out by calculations from the

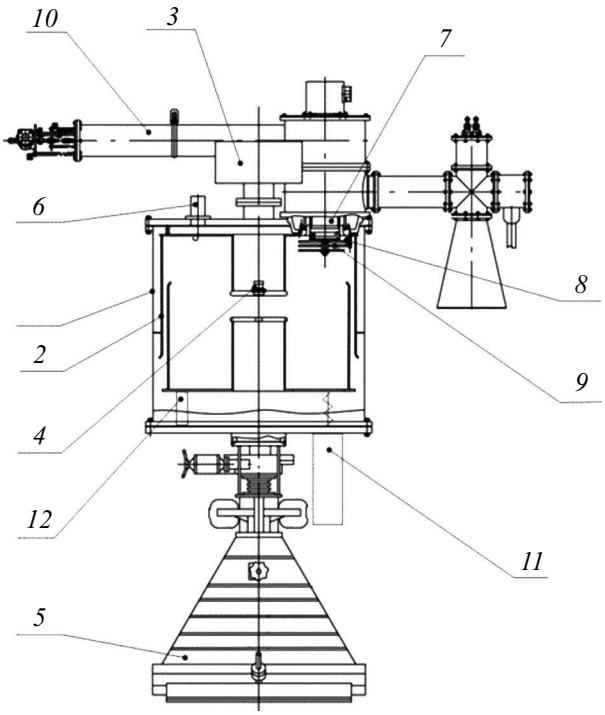

Figure 2. ILU-6 linear accelerator schematic diagram: *1* — vacuum tank; *2* — resonant cavity; *3* — magnetic-discharge pump of NMD type; *4* — electron injector; *5* — output device; *6* — measuring loop; *7* — HF generator lamp anode; *8* — HF power input loop support; *9* — HF power input loop; *10* — cathode loop; *11* — input of shift voltage −7 kV; *12* — supports of lower half of resonant cavity.

parameters of X-ray diffraction patterns using Debye–Scherrer formula:

$$L_C = k\lambda / B\cos\theta, \tag{1}$$

where: L_C — average size of coherent scattering region, nm; k — constant equal to 0.89; B — half-width of diffraction line for reflection angle θ, corresponding to the first diffraction maximum from the set of the lines inherent in each of the identified phases, rad.; λ — wavelength of X-ray CoK_{a_1}-irradiation, nm; $\lambda = 0.178897$ nm.

The density of the study objects was determined in the paper in accordance with the Archimedes law on electronic scale UW620H with an accessory for density measurement. The specimen density was calculated using the following formula:

$$\rho = \rho_0\left(\frac{W_a}{W_a - W_l}\right), \tag{2}$$

where: ρ — specimen density, g/cm^3; ρ_0 — known fluid density, g/cm^3; W_a — specimen weight on air, g; W_l — specimen weight in fluid, g.

X-ray density of hexaferrites was calculated using the data of X-ray diffraction analysis and was in average 5.1 g/cm^3:

$$\rho_{\text{X-ray}} = \frac{2M_A}{VN_A} = \frac{2M_A 2}{ca^2 3\sqrt{3}N_A}, \tag{3}$$

Table 1. Information on $SrFe_{12}O_{19}$ specimens produced in this paper by RTS method

No.	No. of raw blank	No. of specimen	Temperature RTS, °C	Time RTS, min	Density g/cm^3
1.	8-p6	GSI_No. 8	1200	60	4.52
2.	9-p6	GSI_No. 9	1250	60	4.92
3.	11-p6	GSI_No. 11	1300	10	4.95
4.	12-p6	GSI_No. 12	1300	30	4.96
5.	10-p6	GSI_No. 10	1300	60	4.93
6.	13-p6	GSI_No. 13	1300	90	4.93
7.	14-p6	GSI_No. 14	1350	40	4.97
8.	30-p6	GSI_No. 30	1400	304	4.94

where: M_A — molecular mass of hexaferrite; c, a — parameters of elemental cell of hexaferrite; N_A — Avogadro's number, V — elemental cell volume.

Table 1 presents information on the SrM specimens produced in this paper by RTS method.

3. Results and their discussion

Mössbauer spectra of studied samples depending on temperature of synthesis and time (T°C/τ, min: 1200/60; 1250/60; 1300/60; 1350/40) are given in Figure 3.

All specimens were separated in 5 sextets, corresponding to five positions of ions Fe^{3+} in type M hexaferrite structure: 12k, $4f_1$, $4f_2$, 2a and 2b [12]. The produced Mössbauer parameters of sextets after their mathematical processing, isomer shift (δ, mm/s), quadrupolar splitting (Δ, mm/s), magnetic fields on nuclei Fe^{57} (H_{eff}, kOe), width of resonant lines (Γ, mm/s), angle Θ, (degree°) and areas of sextets (S, rel.%) are given in Table 2.

Mössbauer spectrum of specimen 1400/10 is not shown in Figure 3, but Table 2 includes its parameters. From Table 2 one can see that under all processing modes all iron ions comply with valency 3+, according to the values of isomer shift, at the same time all parameters are within the values specified for ions Fe^{3+} of corresponding coordinations: 12k, $4f_2$, 2a — octahedra, $4f_1$ — tetrahedron, and 2b — bipyramide [12]. However, some parameters are slightly different from the theoretical ones. This is true for areas from ions Fe($4f_1$), all specimens, which in certain specimens reach values up to 20.7 rel.% compared to the theoretical 16.7 rel.%. This may be explained by higher probability of resonant effect of tetrahedral ions Fe^{3+}, compared to octahedral ones, as it was explained in paper [13]. On the other hand, one may note the decrease in angle Θ, with temperature increase. This is especially true with reduction of synthesis time (spec. 1350/40, 1400/10). Therefore, under these modes, reduction of angle Θ from 55° leads to increase of specimen magnetic structure.

To find out the effect of directly the synthesis time, Mössbauer spectra of hexaferrites $SrFe_{12}O_{19}$, produced using RTS technology at temperature 1300°C and synthesis

Table 2. Parameters of Mössbauer spectra of isotropic hexaferrites $SrFe_{12}O_{19}$, produced by method of radiation-thermal sintering at different temperature

Specimen $SrFe_{12}O_{19}$, T °C/τ min	Components of spectrum	δ, mm/s	Δ, mm/s	H_{eff}, kOe	S, %	Γ, mm/s	Θ, °
1200/60	C1(12k)	0.35	0.39	412	49.0	0.29	55.3
	C2($4f_2$)	0.37	0.30	517	16.2	0.25	
	C3($4f_1$)	0.26	0.17	491	20.5	0.28	
	C4(2a)	0.34	−0.03	508	7.2	0.22	
	C5(2b)	0.28	2.21	408	7.1	0.30	
1250/60	C1(12k)	0.35	0.40	412	49.4	0.30	55.1
	C2($4f_2$)	0.37	0.30	517	15.5	0.24	
	C3($4f_1$)	0.26	0.17	491	20.5	0.29	
	C4(2a)	0.35	−0.04	508	7.8	0.24	
	C5(2b)	0.28	2.22	408	6.8	0.29	
1300/60	C1(12k)	0.35	0.40	412	49.3	0.30	51.0
	C2($4f_2$)	0.37	0.32	518	15.9	0.25	
	C3($4f_1$)	0.26	0.17	492	20.6	0.29	
	C4(2a)	0.35	−0.04	507	7.8	0.26	
	C5(2b)	0.29	2.21	408	6.4	0.31	
1350/40	C1(12k)	0.35	0.40	412	49.1	0.30	49.3
	C2($4f_2$)	0.37	0.32	517	16.7	0.26	
	C3($4f_1$)	0.26	0.17	491	20.7	0.29	
	C4(2a)	0.35	−0.05	508	7.2	0.22	
	C5(2b)	0.298	2.22	408	6.3	0.29	
1400/10	C1(12k)	0.35	0.40	412	48.6	0.29	49.1
	C2($4f_2$)	0.37	0.31	517	16.4	0.25	
	C3($4f_1$)	0.26	0.17	491	21.4	0.28	
	C4(2a)	0.35	−0.03	507	7.8	0.23	
	C5(2b)	0.29	2.22	408	5.8	0.25	

Table 3. Parameters of Mössbauer spectra of isotropic hexaferrites $SrFe_{12}O_{19}$, produced by RTS method at various values of sintering time

Specimen $SrFe_{12}O_{19}$, T °C/τ min	Components of spectrum	δ, mm/s	Δ, mm/s	H_{eff}, kOe	S, %	Γ, mm/s	Θ, °
1300/10	C1(12k)	0.35	0.39	412	48.8	0.29	52.3
	C2($4f_2$)	0.37	0.31	517	16.2	0.24	
	C3($4f_1$)	0.26	0.18	491	20.9	0.28	
	C4(2a)	0.35	0.04	508	,7.3	0.22	
	C5(2b)	0.29	2.22	407	6.8	0.28	
1300/30	C1(12k)	0.35	0.40	412	49.0	0.28	49.3
	C2($4f_2$)	0.37	0.32	517	16.5	0.24	
	C3($4f_1$)	0.26	0.18	492	20.9	0.27	
	C4(2a)	0.35	−0.02	508	7.8	0.23	
	C5(2b)	0.29	2.21	408	5.8	0.25	
1300/60	C1(12k)	0.35	0.40	412	49.3	0.30	51.0
	C2($4f_2$)	0.37	0.32	518	15.9	0.25	
	C3($4f_1$)	0.26	0.17	492	20.6	0.29	
	C4(2a)	0.35	−0.04	507	7.8	0.26	
	C5(2b)	0.29	2.21	408	6.4	0.31	
1300/90	C1(12k)	0.35	0.40	411	49.5	0.29	49.2
	C2($4f_2$)	0.37	0.31	517	17.0	0.25	
	C3($4f_1$)	0.26	0.17	491	20.6	0.28	
	C4(2a)	0.34	−0.03	508	7.2	0.22	
	C5(2b)	0.29	2.23	408	5.7	0.26	

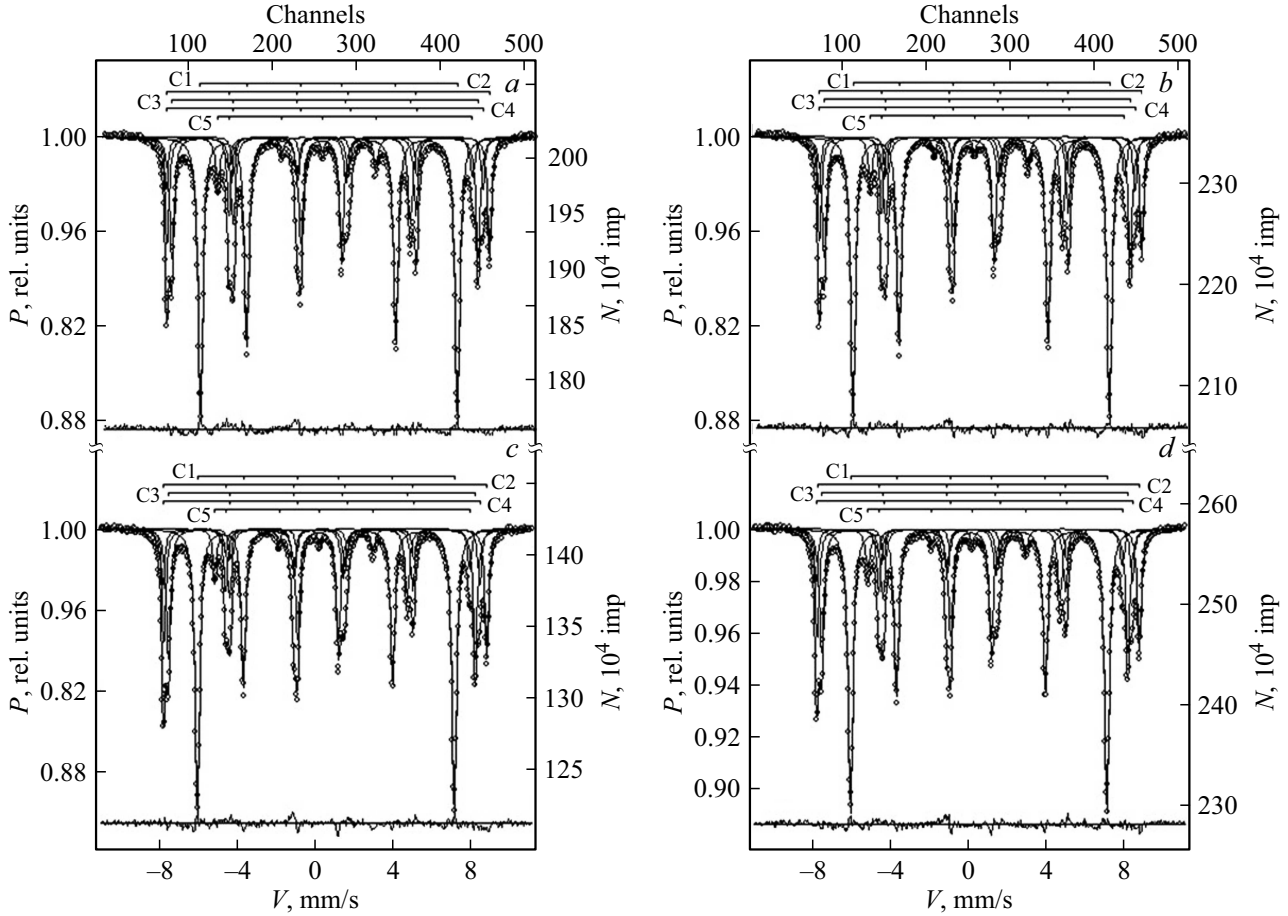

Figure 3. Mössbauer spectra of isotropic hexaferrites $SrFe_{12}O_{19}$, produced by method of radiation-thermal sintering at various values of temperature and time of sintering ($T^{\circ}C/\tau$, min): *a* — 1200/60; *b* — 1250/60; *c* — 1300/60; *d* — 1350/40.

Table 4. Differences in areas of sextets ΔS with opposite directions of magnetic moments of ions Fe^{3+} 12k, 2a, 2b and $4f_1$, $4f_2$

T/τ	1200/60	1250/60	1300/60	1350/40	1400/30	1300/10	1300/30	1300/90
ΔS	26.6	28.0	27.0	30.2	24.4	24.4	25.2	24.4

times 10, 30, 60 and 90 min (Figure 4) were directly registered. Table 3 provides the parameters of the obtained Mössbauer spectra.

From the data provided one can see that as synthesis time increases, angle Θ decrease is observed, but there is no clear dependence of influence thereupon. Besides, the least influence at angle Θ occurs at 10 min synthesis time (specimen 1300/10).

To compare the specific magnetization of specimens with data of Mössbauer measurements, differences of sextet areas ΔS were calculated with the opposite directions of magnetic moments of ions Fe^{3+} 12k, 2a, 2b and $4f_1$, $4f_2$. Differences ΔS are proportionate to specific magnetization in virtue of the fact that it is related both with the total content of iron in the specimen and its localization in the sublattices, which makes it possible to determine the Mössbauer measurements. The calculation results are shown in Table 4.

From the given data of Table 4 one should expect the maximum specific magnetization of specimen 1350/40, and minimum magnetization of specimens 1400/30, 1300/10 and 1300/90, showing the minimum of ΔS, and, accordingly, the worst synthesis mode. The produced maximum value of the difference in areas from iron ions given above for specimen 1250/60, indicates that one should expect the maximum magnetization therefor.

Figure 5 presents X-ray diffraction spectra of specimens of isotropic polycrystalline hexaferrites $SrFe_{12}O_{19}$ GSI_8 (*a*), GSI_9 (*b*) and GSI_10 (*c*), received by RTS method at the following values of temperature and time $T^{\circ}C/\tau$ min: 1200/60; 1250/60 and 1300/60 accordingly. Detailed analysis of X-ray diffraction spectra made it possible to

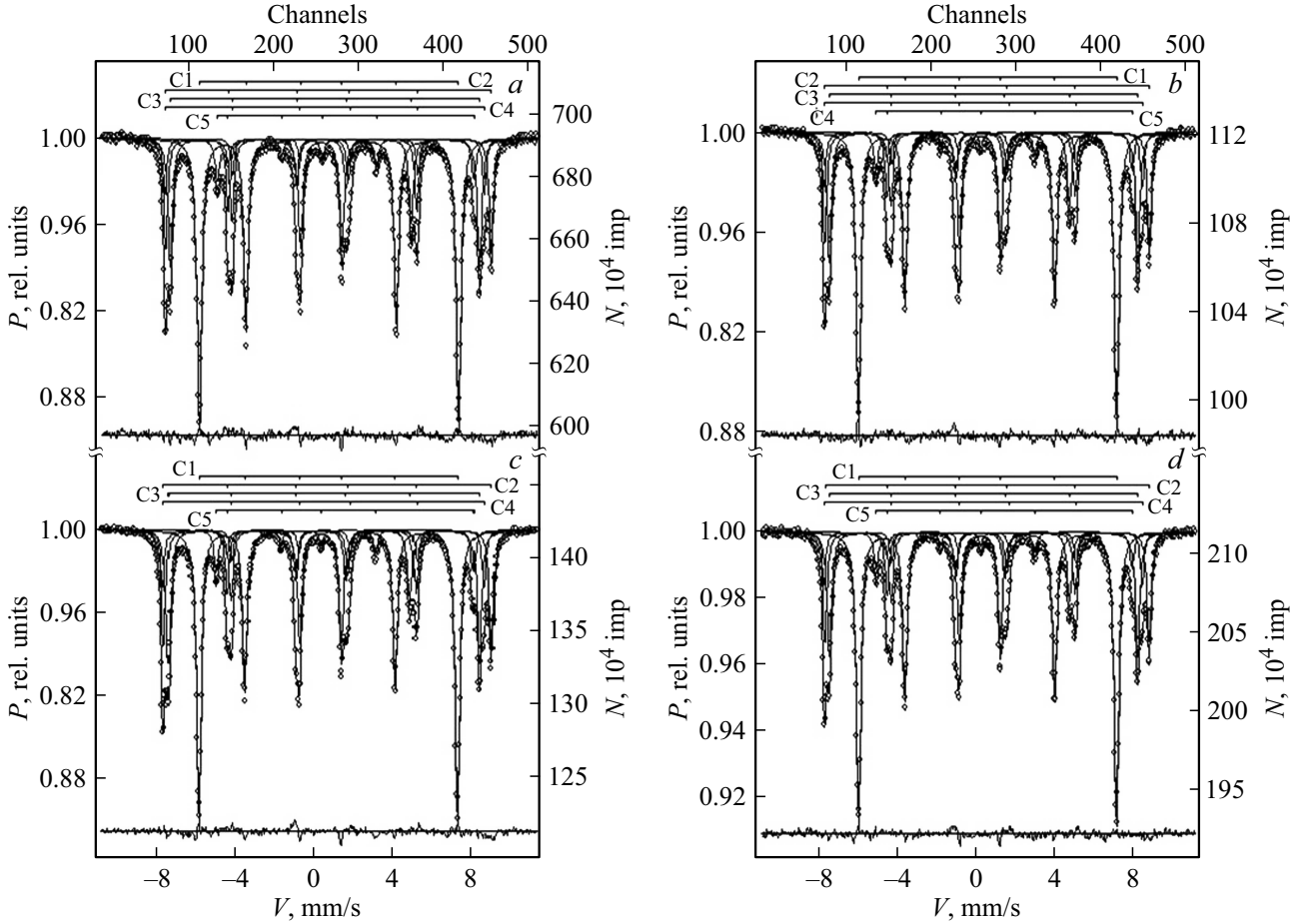

Figure 4. Mössbauer spectra of isotropic hexaferrites $SrFe_{12}O_{19}$, produced by RTS method at 1300°C and various values of sintering time (min): *a* — 10, *b* — 30, *c* — 60, *d* — 90.

establish for some specimens (GSI_No. 9, GSI_No. 10 and especially GSI_No. 12) there was a change in the ratio of intensities in remote corners, which may certify certain features of microstructure. Such behavior may be the result of either crystallite defects, or certain orientation of their growth.

At the fixed sintering time ($\tau = 60$ min) as temperature increases from 1200 to 1300°C, the parameters and volume of the elemental cell of specimens $SrFe_{12}O_{19}$ vary nonlinearly (Figure 6). Minimum values of parameters and volume were noted for specimen GSI_No. 9 (1250°C), which may be due to the effect of microstructure evolution in the sintering process.

Figure 7 presents the dependence of density ρ of isotropic hexaferrite specimens $SrFe_{12}O_{19}$ if produced using RTS technology on sintering time at RTS temperature = 1300°C (*a*) and RTS temperature at sintering times $\tau = 30$ min and $\tau = 60$ min (*b*). It is characteristic that density $SrFe_{12}O_{19}$ decreases with increase in RTS time (at RTS temperature 1300°C) and increases with RTS temperature increase within the used values of temperature and time of RTS.

It should be noted that some results above obtained by us for strontium hexaferrite $SrFe_{12}O_{19}$ were previously obtained for other ferrite materials [7–9,14–22], especially for barium hexaferrite $SrFe_{12}O_{19}$ [14]. The fact that RTS technology allows ferrite sintering within several dozens of minutes is quite interesting. And the prevailing role in this process belongs specifically to RTS temperature value, which is — specific for every type of ceramics. Currently the physical mechanism of intensification of the ceramics sintering process when exposed to fast electron flux has not yet been fully understood [15–18]. The opinion that is most common and established in the experts' circle is that the prevailing mechanism of radiative gain of mass transfer in ferrite ceramics is surface-recombination mechanism. When ceramic stocks are irradiated, electron excitations are induced in grains and powder pressed pieces that attempt to localize at the boundaries of grains, phases, and to recombine there, releasing energy and heat. As a result of the specified processes, temperature gradients are developed, which cause thermal diffusion fluxes that substantially contribute to acceleration of ferrite solid phase synthesis reactions.

4. Conclusions

Therefore, this paper for the first time synthesized isotropic polycrystalline hexagonal ferrites $SrFe_{12}O_{19}$ by RTS method. Magnetic and crystalline structures were studied, as well as some physical properties of the produced study objects. Our findings suggest the following conclusions.

1. The specimens $SrFe_{12}O_{19}$ produced by RTS method in the paper were single-phase.

2. RTS may be used as alternative technology to produce a hexagonal ferrite $SrFe_{12}O_{19}$. Compared to the traditional

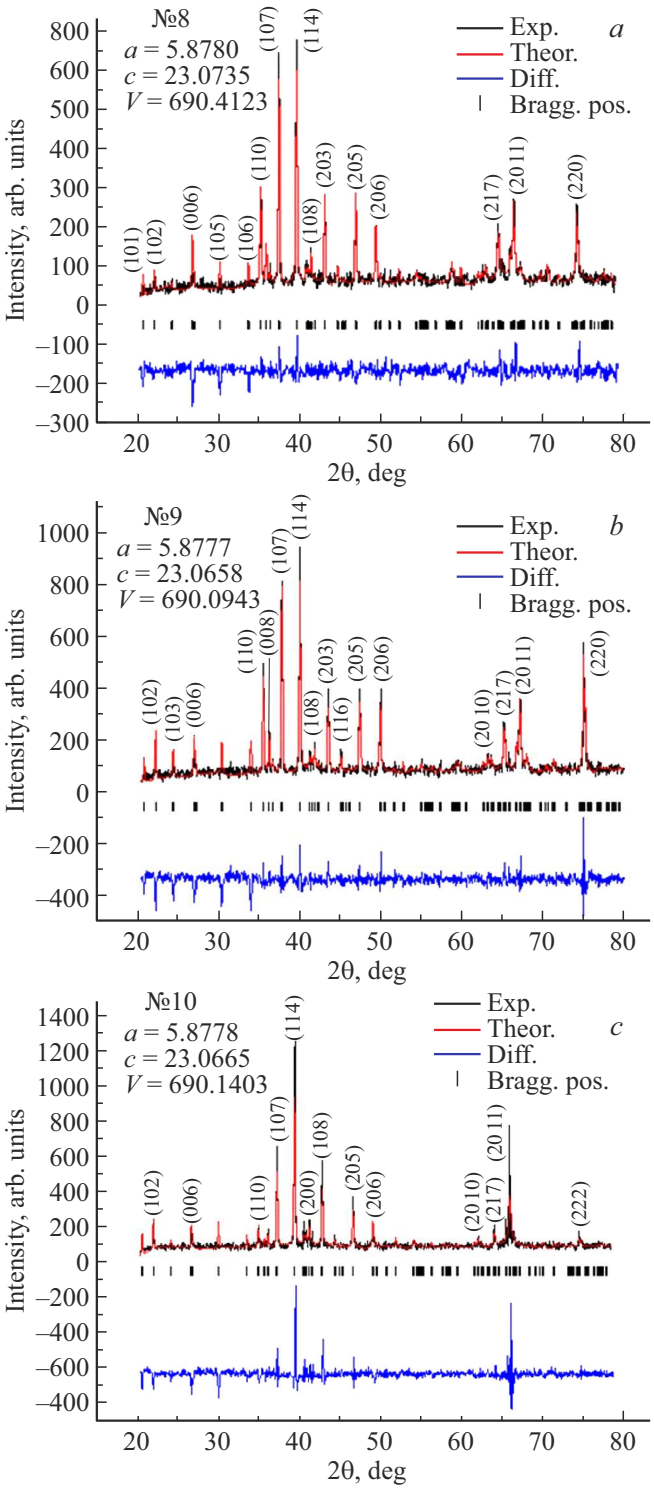

Figure 5. X-ray diffraction spectra of isotropic polycrystalline hexaferrite specimens $SrFe_{12}O_{19}$ GSI_8 (*a*), GSI_9 (*b*) and GSI_10 (*c*), received by RTS method.

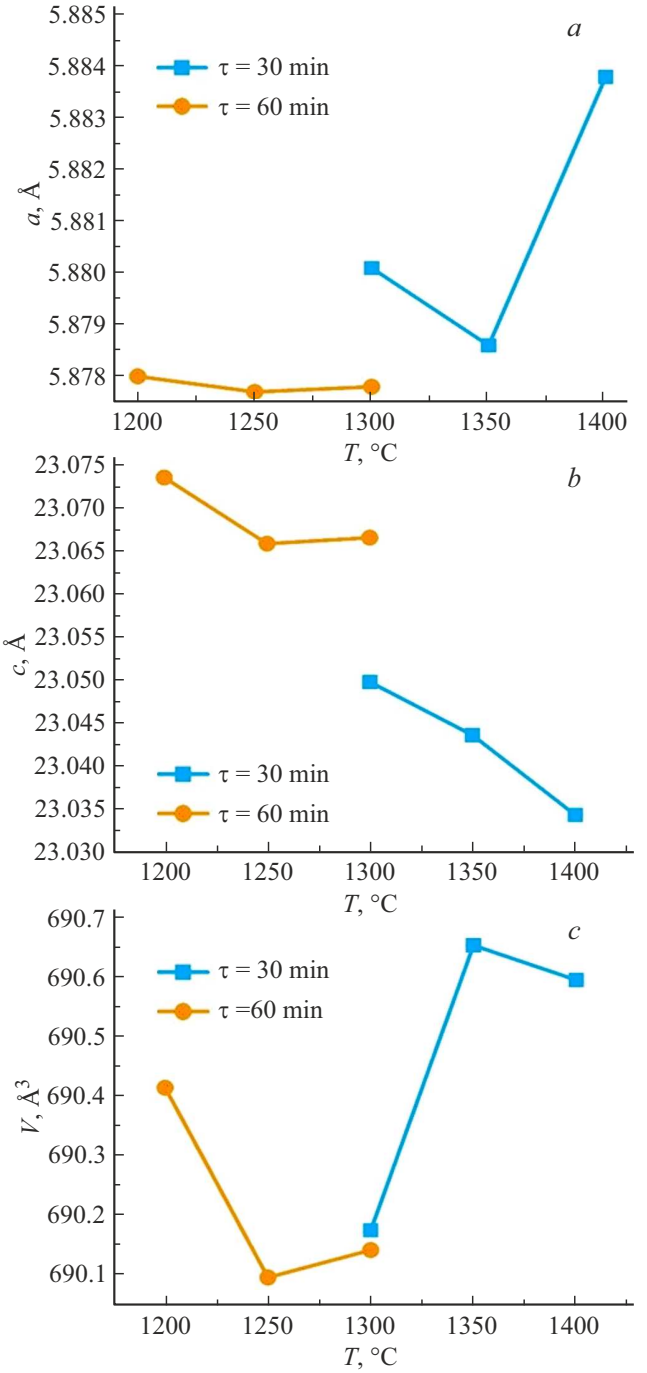

Figure 6. Variation of parameters of lattice *a* (*a*), *c* (*b*) and volume *V* (*c*) of elemental cell for specimens of isotropic polycrystalline hexaferrites $SrFe_{12}O_{19}$, synthesized by RTS at various temperatures for 60 and 30 min.

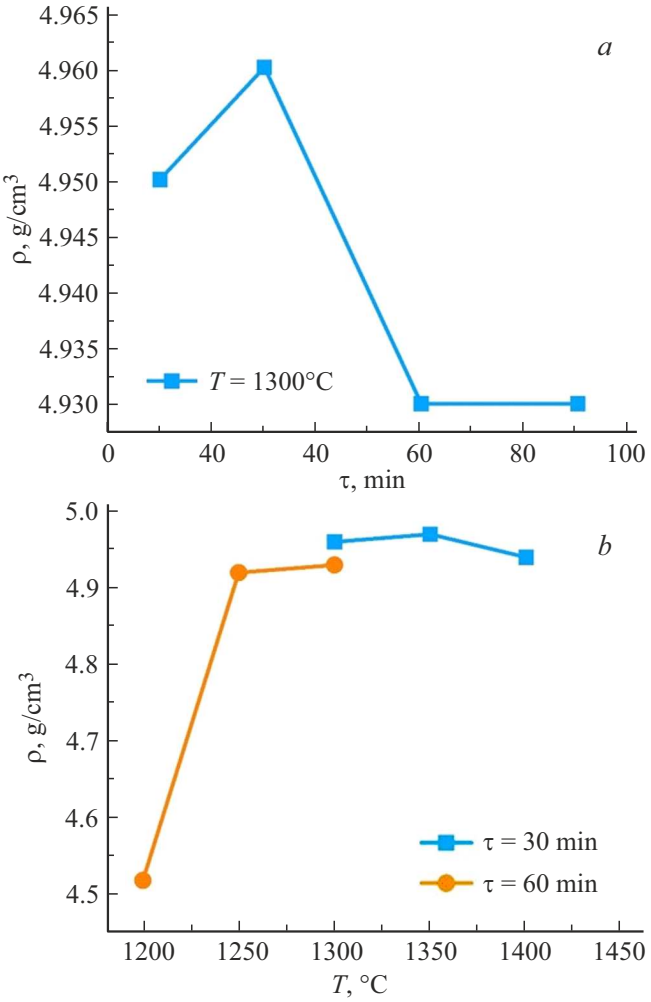

Figure 7. Variation in density of hexaferrite specimens $SrFe_{12}O_{19}$ at RTS depending on RTS time (*a*) and RTS temperature (*b*).

ceramic technology with thermal sintering, RTS technology proved itself to be a highly energy-efficient and inexpensive.

3. In RTS technology the sintering temperature values plays a substantially larger role compared to the sintering time value.

4. In process of RTS of hexaferrites $SrFe_{12}O_{19}$ anisotropic distortion of elemental cell was most probably due to the inductance of oxygen vacancies in the crystalline lattice by fast electrons. Highly likely, to improve parameters of specimens $SrFe_{12}O_{19}$ it will be necessary to use an additional finish operation of short-term annealing in oxygen atmosphere.

5. The most optimal mode for synthesis of isotropic hexaferrites $SrFe_{12}O_{19}$ is the range 1250−1300°C and sintering time 30−60 min.

Funding

The study was completed using project funds of the Russian Science Foundation No. 24-13-00268

Conflict of interest

The authors declare that they have no conflict of interest.

References

[1] L.M. Letyuk, V.G. Kostishin, A.V. Gonchar. Tekhnologiya ferritovykh materialov magnitoelektroniki. MISIS, M. (2005). 352 s. (in Russian).
[2] A.B. Altman, A.N. Gerber, P.A. Gladyshev, Yu.A. Gratsianov, E.N. Zeyn, L.A. Kavalerova, Yu.M. Pyatin, Yu.S. Sakatunov, V.G. Sergeev, A.D. Skokov, R.Yu. Sukhorukov, A.M. Chernyavskaya. Postoyannye magnity. Spravochnik / Pod. red. Yu.M. Pyatina, 2-e izd., pererab. i dop. Energiya, M. (1980). 488 s. (in Russian).
[3] A. Ustinov, V.N. Kochemasov, E.R. Khasianova. Elektronika NTB **148**, *8*, 86 (2015). (in Russian).
[4] M. Shalaby, M. Peccianti, Y. Ozturk, R. Morandotti. Nature Communications **4**, *1*, 1558 (2013).
[5] R.C. Pullar. Prog. Mater. Sci. **57**, *7*, 1191 (2012).
[6] V.G. Harris. IEEE Transactions on Magnetics **48**, *3*, 1075 (2011).
[7] I.M. Isaev, S.V. Scherbakov, V.G. Kostishin, A.G. Nalogin, V.V. Moklyak, B.K. Ostafiychuk, A.A. Alekseev, V.V. Korovushkin, E.A. Belokon, M.V. Kalinyuk, M.A. Mikhaylenko, M.V. Korobeynikov, A.A. Bryazgin, D.V. Salogub. Izvestiya vysshikh uchebnykh zavedeniy. Materialy elektronnoj tekhniki **20**, *3*, 220 (2017). (in Russian).
[8] V.G. Kostishin, V.V. Korovushkin, A.G. Nalogin, S.V. Scherbakov, I.M. Isaev, A.A. Alekseev, A.Yu. Mironovich, D.V. Salogub. FTT **62**, *7*, 1028 (2018). (in Russian).
[9] A.P. Surzhikov, A.M. Pritulov, E.N. Lysenko, A.N. Sokolovskii, V.A. Vlasov, E.A. Vasendina. Journal of Thermal Analysis and Calorimetry **109**, *1*, 63 (2011).
[10] V.L. Auslender, A.A. Bryazgin, L.A. Voronin, G.B. Glagolev, I.V. Gornakov, E.N. Kokin, G.S. Kraynov, G.I. Kuznetsov, A.N. Lukin, I.G. Makarov, S.A. Maksimov, S.V. Miginsky, V.E. Nekhaev, A.D. Panfilov, V.M. Radchenko, N.D. Romashko, A.V. Sidorov, M.A. Tiunov, V.O. Tkachenko, A.A. Tuvik, B.L. Faktorovich, V.G. Cheskidov. Nauka — proizvodstvu **63**, *7*, 11 (2003). (in Russian).
[11] A.S. Komlev, I.M. Isaev, V.G. Kostishin, D.N. Chitanov, AABV. Timofeev. Yacheyka dlya radiatsionno-termicheskogo spekaniya. NOU-KHAU. Zaregistrirovano v Depozitarii noukhau NITU „MISIS“ No. 81-219-2016 OIS ot 29 dekabrya 2016 g. (in Russian).
[12] X. Obradors, A. Collomb, M. Pernet, D. Samaras, J.C. Joubert. Journal of Solid State Chemistry **56**, *2*, 1191 (2012).
[13] V.G. Kostishin, V.V. Korovushkin, K.V. Pokholok, A.V. Trukhanov, I.M. Isaev, A.Yu. Mironovich, M.A. Darvish. Fizika tverdogo tela **63**, *10*, 1496 (2021). (in Russian).
[14] V.G. Kostishin, I.M. Isaev, S.V. Scherbakov, A.G. Nalogin, E.A. Belokon, A.A. Bryazgin. Vostochno-Evropeyskiy zhurnal peredovykh tekhologiy **5**, *8*, 32 (2016).
[15] A.Yu. Annenkov, A.S. Ivashutenko. Izvestiya Tomskogo politekhnicheskogo universiteta **308**, *7*, 30 (2005). (in Russian).
[16] A.P. Surzhikov, E.N. Lysenko, A.V. Malyshev, A. Petrova, S.A. Ghyngazov, A.K. Aimukhanov. Eurasian Physical Technical Journal **17**, *1*, 26 (2020).
[17] O. Stary, A.V. Malyshev, E.N. Lysenko, A. Petrova. Eurasian Journal of Physics and Technology **17**, *2*, 6 (2020).

[18] A.S. Komlev. Tavricheskiy nauchny obozrevatel **17**, *12*, 135 (2016) (in Russian).
[19] A.V. Malyshev, E.N. Lysenko, E.A. Sheveleva, O.A. Surzhikova, A.K. Aringazin. Materials science **18**, *1*, 3 (2021).
[20] O. Stary, A.P. Surzhikov, A.V. Malyshev, E.N. Lysenko, E.A. Sheveleva. Eurasian Physical Technical Journal **18**, *3*, 11 (2021).
[21] A.P. Surzhikov, A.V. Malyshev, E.N. Lysenko, O. Stary. Materials science **19**, *1*, 5 (2022),
[22] E.N. Lysenko, A.P. Surzhikov, A.V. Malyshev, V.A. Vlasov, E.V. Nikolaev. Izvestiya vuzov. Khimiya i khimicheskaya tekhnologiya **61**, *6*, 69 (2018) (in Russian).

Translated by M.Verenikina